JCTC Journal of Chemical Theory and Computation

Article

pubs.acs.org/JCTC

Molecular Electrical Properties from Quantum Monte Carlo Calculations: Application to Ethyne

Emanuele Coccia,[†] Olga Chernomor,[‡,∥] Matteo Barborini,[‡] Sandro Sorella,[§] and Leonardo Guidoni*[,†]

[†]Dipartimento di Scienze Fisiche e Chimiche, Universitá degli Studi dell'Aquila, via Vetoio (Coppito), 67100, L'Aquila, Italy

[‡]Università Degli Studi de L'Aquila, Dipartimento di Matematica Pura ed Applicata, via Vetoio (Coppito 1), 67100 L'Aquila, Italy

[§]Scuola Internazionale Superiore di Studi Avanzati (SISSA) and Democritos National Simulation Center, Istituto Officina dei Materiali del CNR, via Bonomea 265, 34136 Trieste, Italy

ABSTRACT: We used Quantum Monte Carlo (QMC) methods to study the polarizability and the quadrupole moment of the ethyne molecule using the Jastrow-Antisymmetrised Geminal Power (JAGP) wave function, a compact and strongly correlated variational ansatz. The compactness of the functional form and the full optimization of all its variational parameters, including linear and exponential coefficients in atomic orbitals, allow us to observe a fast convergence of the electrical properties with the size of the atomic and Jastrow basis sets. Both variational results on isotropic polarizability and quadrupole moment based on Gaussian type and Slater type basis sets are very close to the Lattice Regularized Diffusion Monte Carlo values and in very good agreement with experimental data and with other quantum chemistry calculations. We also study the electronic density along the C≡C and C−H bonds by introducing a generalization for molecular systems of the small-variance improved estimator of the electronic density proposed by Assaraf et al. (Assaraf, R.; Caffarel, M.; Scemama, A. *Phys. Rev. E*, **2007**, *75*, 035701).

1. INTRODUCTION

The correct modeling of the electrostatic and dispersive interactions in atomic and molecular systems requires a deep understanding of the electrical properties, such as multipole moments and polarizabilities.[1] Such quantities are strongly dominated by the long-range behavior of the electronic wave function. Two ingredients in quantum chemistry calculations are crucial to assess a reliable and meaningful description of the electrical properties:[2] the correct inclusion of correlation effects and the use of a large basis set, including several polarization and diffuse terms in the description of the atomic orbitals. For this reason the accurate evaluation of these properties can be still a challenge for large molecular systems. In the present work we perform a systematic study of molecular electrical properties by means of Quantum Monte Carlo (QMC) methods,[3−8] which represent a powerful tool to solve electronic many-body problems.

The Variational Monte Carlo (VMC) consists of the stochastic integration of the expectation value of the Hamiltonian on a given ansatz wave function. Correlated many-body wave functions used in VMC have a given functional form, determined by a finite (large) number of variational parameters usually obtained through an optimization procedure, with a statistical iterative technique that is converging to the lowest variational many-body wave function for the system. One advantage of this approach is that wave function parametrizations that go beyond the usual expansion in Slater determinants can be often implemented in a simple way and without significant computational overload. In particular, electronic correlation can be described through the Jastrow factor, a bosonic term (positive and symmetric under electron permutations) depending explicitly on the electronic and nuclear positions. Another group of QMC methods is based on the stochastic solution of the Schrödinger equation through projection techniques. For instance in the Diffusion Monte Carlo (DMC) technique, the ground state component of a given trial function is extracted by a long enough imaginary time diffusion process. DMC allows one to obtain the exact ground-state energy of the system,[3,4,7] within the so-called fixed-node approximation.[9] QMC methods have been successfully applied to study different systems such as materials,[4,10−12] hydrogen bonding[13] and van der Waals[14] networks, and electronic excitations in the gas phase[8,15,16] and within a QM/MM approach.[17]

The parametrization of the variational wave function has rapidly evolved in recent years, leading to several systems with an accurate description of the electronic correlation already at the VMC level. In particular, a modern and fully correlated implementation of Pauling's valence bond idea was recently introduced by one of us and collaborators: the Jastrow Antisymmetrised Geminal Power (JAGP).[18−20] The compactness of this functional form combined with the use of effective methods for the optimization of all parameters, including linear coefficients and exponents of the atomic basis sets,[14,21,22] leads to a rapid convergence of the variational results for electronic and geometrical properties with the size of the basis sets.[8,23] The reduced number of variational parameters together with the good description of the electronic correlation effects make the Quantum Monte Carlo methods, in combination with JAGP wave functions, good candidates for an accurate evaluation of electrical molecular properties.

QMC calculations of molecular electronic polarizabilities have been so far limited to the case of the H atom.[24] In the present work, we propose to study by QMC the electrical properties of ethyne (HCCH), a simple molecule widely

Received: February 29, 2012
Published: April 23, 2012

studied both from an experimental and theoretical standpoint over the years, with a large number of data available for multipole moments and for (hyper)polarizabilities.[2,25−47] This system can be considered a prototype for the theory and for the application of different computational strategies due to its large polarizability; at the same time, it represents the simplest molecule with a triple bond between carbon atoms.

Gas-phase Rayleigh elastic scattering and Raman inelastic scattering measurements, together with dipole (e,e) spectroscopy, give a direct estimation of the dipole polarizability[42] between 22.3[26] and 23.53(25) au;[42] a larger value of 26.5 au is instead given from a dielectric constant measure.[27,42] On the other hand, HF calculations estimate the pure electronic polarizability of HCCH[2,34] with a value of 23.11 au[31] and 22.716 au;[2] while correlated methods, like MP2 and CCSD schemes, converge, respectively, to 22.711 au and to 22.52 au.[2,34,42] The above results do not take into account the zero-point contribution to polarizability, which has been estimated to be about 0.5 au,[2] depending on the chosen basis set.

Experiments for detecting the quadrupole moment are based on the Cotton-Mouton effect,[30,37] field gradient-induced birefringence,[40] and collision-induced far-infrared absorption[32] and produce a quite large range of values, from 4.48 to 5.57 au.[43,44,46] Theoretical estimates from correlated methods (MP4 and CCSD(T)), together with DFT results, converge to 4.8−4.9 au,[35,39,43,44,46] whereas HF calculations are largely inaccurate;[2,41,43,44,46] vibrational corrections taking into account the zero-point energy of the lowest vibrational eigenstate are small (ranging from 0.04 to 0.08 au) and can be neglected.[2]

We study the dipole polarizability and the quadrupole moment of ethyne using JAGP wave functions differing in the size and in the shape (Gaussian-type or Slater-type orbitals) of the atomic basis sets for both the Jastrow and determinantal part. The electronic density profile along the triple C≡C bond and the C−H bond is calculated by an extension of the method introduced by Assaraf et al.[48] In section 2 we review the basics of the Variational Monte Carlo and Lattice Regularized Diffusion Monte Carlo (LRDMC),[49,50] and we explain the functional form of the trial wave function used and the way through which we estimate the properties of interest; we therefore describe in detail the improved density estimator. Section 3 collects the computational strategy together with the basis sets employed in the calculations, while in section 4 we report our VMC and LRDMC results comparing them with those from other computational techniques and experiments. Finally, in the Conclusions we summarize our findings and underline the new perspectives for QMC methods to become standard tools for electronic structure simulations, thanks to the fact that much smaller basis sets are required to achieve an accuracy comparable with state of the art post Hartree−Fock approaches. This looks very promising for future extension of QMC to much larger systems, as the computer time required to employ VMC scales with a relatively small power p of the number of electrons: $p = 2$ for bulk properties and $p = 4$ for quantum chemistry calculations with fixed accuracy in the total energy.

2. QUANTUM MONTE CARLO

2.1. VMC and LRDMC. The Variational Monte Carlo (VMC) energy E_{VMC} is represented as the minimum of the expectation value of the electronic Hamiltonian $\hat{H}$, over the variational parameters $\mathbf{p} = \{p_i\}$ of a trial wave function Ψ_T, given a specific nuclear configuration $\mathbf{R}$:

$$E_{VMC} = \min_{\mathbf{p}} E[\Psi_T(\mathbf{p}, \mathbf{R})] \tag{1}$$

where

$$E[\Psi_T] = \langle \hat{H} \rangle_{\Psi_T^2} = \frac{\int \Psi_T(\mathbf{x}) \hat{H} \Psi_T(\mathbf{x})\, d\mathbf{x}}{\int \Psi_T^2(\mathbf{x})\, d\mathbf{x}} \tag{2}$$

In VMC,[3] the latter integral over the collective electronic coordinate $\mathbf{x}$ is written in terms of the local energy, defined as $E_L = \hat{H}\Psi_T/\Psi_T$, and of a probability density $|\Psi_T^2|/\int|\Psi_T^2|$ (in eq 2 and in the following, the parametric dependence of Ψ_T on $\mathbf{p}$ and $\mathbf{R}$ will be omitted).

$$E[\Psi_T] = \frac{\int \Psi_T^2(\mathbf{x}) E_L(\mathbf{x})\, d\mathbf{x}}{\int \Psi_T^2(\mathbf{x})\, d\mathbf{x}} \tag{3}$$

The value of the integral in eq 3 is then estimated as a sum over a set of points $\mathbf{x}$ in the configurational space of the $6N$ electronic Cartesian and spin coordinates, generated stochastically according to the probability density $((|\Psi_T^2|)/(\int|\Psi_T^2|))$. The optimization procedure is based on the linear optimization method described in refs 14 and 22.

The Lattice Regularized Diffusion Monte Carlo (LRDMC) method is a projection QMC technique, in which the Schrödinger equation is solved through a relaxation process in imaginary time exploiting the discretization of the electronic Hamiltonian on a lattice grid with a step equal to a.[49,50]

2.2. Variational Resonating Valence Bond Wave Function. As already introduced, the trial wave function used in this investigation is the Jastrow Antisymmetrised Geminal Power (JAGP),[19,20] inspired by Pauling's resonance valence bond (RVB) approach.[51] The JAGP is built as the product between an Antisymmetric Geminal Power (AGP)[52,53] and a Jastrow factor $J(\mathbf{r})$

$$\Psi_T(\mathbf{x}) = \Psi_{AGP}(\mathbf{x}) J(\mathbf{r}) \tag{4}$$

and includes both static and dynamical electron correlation effects;[13,14,54,55] J is independent of spin coordinates to avoid spin contamination.[19,56]

For molecular systems of N electrons and M nuclei in a spin singlet state, i.e., $N/2 = N^{\uparrow} = N^{\downarrow}$, the AGP is written as

$$\Psi_{AGP}(\mathbf{x}) = \hat{A} \prod_{i}^{N/2} \Phi_G(x_i^{\uparrow}; x_i^{\downarrow}) \tag{5}$$

where $\mathbf{x}$ is the set of Cartesian and spin coordinates of the N electrons, $\hat{A}$ is the antisymmetrization operator, and Φ_G is the Geminal pairing function defined as

$$\Phi_G(\mathbf{x}_i; \mathbf{x}_j) = \phi_G(\mathbf{r}_i, \mathbf{r}_j) \frac{1}{\sqrt{2}} (|\uparrow\rangle_i |\downarrow\rangle_j - |\uparrow\rangle_j |\downarrow\rangle_i) \tag{6}$$

Φ_G is given by a singlet spin function multiplied by a spatial part $\phi_G(\mathbf{r}_i, \mathbf{r}_j)$, which is a linear combination of products of atomic orbitals:

$$\phi_G(\mathbf{r}_i, \mathbf{r}_j) = \sum_{A,B}^{M} \sum_{\mu,\nu} \lambda_{\mu_A \nu_B} \psi_{\mu_A}(\mathbf{r}_i) \psi_{\nu_B}(\mathbf{r}_j) \tag{7}$$

where the indexes μ and ν run over the basis sets centered on the Ath and Bth nuclei.

These pairing (valence bond) functions couple electrons belonging to different atoms according to the $\lambda_{\mu_A \nu_B}$ coefficients.

In case of electronic states with unpaired electrons, the above scheme has been generalized.[19,20]

The Jastrow term J[57] introduces dynamic correlation effects, and it enforces the fulfillment of electron−electron and electron−nucleus cusp conditions.[56] In JAGP, it is written as the product of four terms, $J = J_1J_2J_{3,4}$. The first term J_1 is the so-called one-body Jastrow factor:

$$J_1(\mathbf{R}, \mathbf{r}) = \exp\left\{\sum_{A,i} -(2Z_A)^{3/4}\xi((2Z_A)^{1/4}r_{iA}) + \Xi_A(\mathbf{r}_i)\right\} \tag{8}$$

where $\mathbf{r}_{iA} = |\mathbf{r}_i - \mathbf{R}_A|$ is the distance between the ith electron and the Ath nucleus, Z_A is the nuclear charge (pseudo charge in presence of pseudopotentials), and M is the number of atoms in the molecule. This factor includes both the homogeneous interaction between the electron and the nuclei through the function $\xi(r) = B/2(1 - e^{-r/B})$, and the nonhomogeneous term built from the linear combination of atomic orbitals $\Xi_A(\mathbf{r}_i) = \sum_{\mu_A} g_{\mu_A}\chi_{\mu_A}(\mathbf{r}_i)$.

The second term is the purely homogeneous electron−electron two-body factor

$$J_2(\mathbf{r}) = \exp\{\sum_{i<j}^{N} \xi(r_{ij})\} \tag{9}$$

that depends only on the distances $r_{ij} = |\mathbf{r}_i - \mathbf{r}_j|$ between any electron pair, treating the electron−electron cusp conditions of the JAGP wave function through the function $\xi(r_{ij}) = b/2(1 - e^{-r_{ij}/b})$.

The last terms are the three- and four-body Jastrow J_3 and J_4 that include the electron−electron-nuclei correlations

$$J_{3,4}(\mathbf{r}) = \exp\left\{\sum_{i<j}^{N} \varpi(\mathbf{r}_i, \mathbf{r}_j)\right\} \tag{10}$$

where

$$\varpi(\mathbf{r}_i, \mathbf{r}_j) = \sum_{A,B}^{M} \sum_{\mu_A\nu_B} g_{\mu_A\nu_B}\chi_{\mu_A}(\mathbf{r}_i)\chi_{\nu_B}(\mathbf{r}_j) \tag{11}$$

Terms with $A = B$ represent the three-body term, whereas terms with $A \neq B$ are four-body terms, which describe the dynamical correlation of electrons on different atomic centers.

2.3. Polarizability and Quadrupole. In the VMC framework, the expectation value of a generic operator $\hat{O}(\mathbf{r},\mathbf{R})$, a function of the electronic and nuclear coordinates, is calculated as the average over the random walks W

$$\frac{\langle\Psi_T|\hat{O}|\Psi_T\rangle}{\langle\Psi_T|\Psi_T\rangle} = \langle\hat{O}\rangle_{\Psi_T^2} \equiv \langle\hat{O}\rangle_v \sim \frac{1}{W}\sum_{i}^{W} O(\bar{\mathbf{r}}_i, \mathbf{R}_i) \tag{12}$$

The energy for a neutral $D_{\infty h}$ molecule embedded in a static external electric field can be written as a Taylor expansion:[58]

$$E = E^0 - \frac{1}{2}\alpha_{\alpha\beta}F_\alpha F_\beta - \frac{1}{3}\Theta_{\alpha\beta}F_{\alpha\beta} - \frac{1}{6}C_{\alpha\beta,\gamma\delta}F_{\alpha\beta}F_{\gamma\delta}\cdots \tag{13}$$

where α and β subscripts are the Cartesian coordinates, F_α is the applied electric field, $F_{\alpha,\beta}$ is the field gradient at the expansion point, E^0 and Θ are the energy and the quadrupole moment tensor of the molecule at $\mathbf{F} = 0$, α and C are, respectively, the dipole and quadrupole polarizability tensors.[59] For linear molecules, with the z axis coinciding with the molecular axis, the definition of the quadrupole moment Θ and the dipole polarizability α does not depend on the origin of the reference frame; for the case of the ethyne, both tensors are diagonal. In addition, because of the cylindric symmetry, the polarizability tensor has only two independent components and we can define the spherical average of the α tensor $\bar{\alpha}$ and the measure of its anisotropy $\Delta\alpha$ as follows:

$$\bar{\alpha} = \frac{\alpha_{zz} + 2\alpha_{xx}}{3} \tag{14}$$

$$\Delta\alpha = \alpha_{zz} - \alpha_{xx} \tag{15}$$

We adopted a finite-field approach[58] to evaluate polarizabilities by the derivative of the molecular dipole with respect to the external field:

$$\alpha_{\alpha\alpha} = \left(\frac{\partial\mu_\alpha}{\partial F_\alpha}\right)_{F_\alpha=0} \sim \frac{\mu_\alpha(F_\alpha) - \mu(-F_\alpha)}{2F_\alpha} \tag{16}$$

By applying a constant perturbing field of 0.01 au and a three-point central difference approximation (with errors of order F_α^2), we can estimate the value of the $\alpha_{\alpha\alpha}$ component from VMC calculations by averaging the value of the dipole components, e.g., $\mu_\alpha = \langle\mu_\alpha\rangle_{\Psi_T^2} = (1/W)\sum_i^W \mu_\alpha(\bar{\mathbf{r}}_i)$, for various fields. Since finite differences estimators are critical in QMC methods because the errors blow up in the finite difference limit, it would be desirable within our approach to use the largest possible value for the external field. To this purpose we preliminary investigated with a DFT/B3LYP study (TZVP basis sets (10s6p)/[6s3p] for C and (5s)/[3s] for H, with the addition of polarization and diffuse functions) the linear response regime of the electronic density with respect to the external field, finding a linear response with 0.01 au. We therefore used this value to calculate polarizabilities in order to minimize the error due to the finite difference approach.

The $\Theta_{\alpha\beta}$ component of the quadrupole is defined, for a molecular system of N electrons and M nuclei, as

$$\Theta_{\alpha\beta} = \frac{1}{2}[-\sum_{i}^{N}(3r_{i\alpha}r_{i\beta} - r_i^2\delta_{\alpha\beta}) + \sum_{A}^{M} Z_A(3R_{A\alpha}R_{A\beta} - R_A^2\delta_{\alpha\beta})] \tag{17}$$

where $\mathbf{r}_{i\alpha}$ is the α Cartesian component of the ith electron, $R_{A\alpha}$ is the analogous for the nuclei, and Z_A is the nuclear charge. The tensor is traceless and is characterized by only one independent component. The isotropic estimate Θ_{eff} of the quadrupole is given by

$$\Theta_{eff} = \sqrt{\frac{2}{3}[\Theta_{xx}^2 + \Theta_{yy}^2 + \Theta_{zz}^2]} \tag{18}$$

with each $\Theta_{\alpha\alpha}$ being the VMC average over the random walks, $\Theta_{\alpha\alpha} = \langle\Theta_{\alpha\alpha}\rangle_{\Psi_T^2} = (1/W)\sum_i^W\Theta_{\alpha\alpha}(\bar{\mathbf{r}}_i)$.

LRDMC estimates have been calculated using the well-known mixed estimator according to which property of interest is averaged over the mixed distribution given by $\Psi_T\Phi_{FN}$, where Φ_{FN} is the exact ground-state wave function within the fixed node (FN) approximation.[3]

2.4. Electronic Density. The electronic density can be directly calculated by the stochastic sampling accumulated in the VMC scheme using the following estimator:

$$\rho(\mathbf{r}) = \langle \sum_i^N \delta(\mathbf{r}_i - \mathbf{r}) \rangle_{\Psi_T^2} \tag{19}$$

where $\delta(\mathbf{r}_i - \mathbf{r})$ is the δ Dirac function. In practice, the set of discrete points $\mathbf{r}_i$ of the random walk are accumulated on a 3D grid. The use of a coarse grid can give a poor spatial description of density variations, whereas the use of an excessively fine grid may have small statistics per point (i.e., large errors); moreover, in regions with very low sampling or no sampling points, there is no possibility to get a reasonable evaluation of the density, independently of the grid spacing. To alleviate the above drawback, Assaraf et al. have presented a general improved density estimator[48] based on the differential identity for the δ function:

$$\delta(\mathbf{r}_i - \mathbf{r}) = -\frac{1}{4\pi}\nabla_i^2 \frac{1}{|\mathbf{r}_i - \mathbf{r}|} \tag{20}$$

The density estimator can be therefore written as

$$\rho(\mathbf{r}) = \left\langle \sum_i^N -\frac{1}{4\pi}\nabla_i^2 \frac{1}{|\mathbf{r}_i - \mathbf{r}|} \right\rangle_{\Psi_T^2} \tag{21}$$

which is shown in ref 48 to be equivalent to

$$\rho(\mathbf{r}) = \left\langle -\frac{1}{4\pi} \sum_i^N \frac{1}{|\mathbf{r}_i - \mathbf{r}|} \frac{\nabla_i^2 \Psi_T^2(\mathbf{r}_1, ..., \mathbf{r}_N)}{\Psi_T^2(\mathbf{r}_1, ..., \mathbf{r}_N)} \right\rangle_{\Psi_T^2} \tag{22}$$

The great advantage of the density definition in eq 22 is that, despite the quality of the Monte Carlo sampling, it will have a smooth finite value in each point $\mathbf{r}$, including those regions never visited by the Monte Carlo random walk. Two main drawbacks still arise from the definition given by eq 22:[48] (i) the variance of the estimator is unbounded in the neighborhood of the nuclei because of the presence of the derivative $(\nabla_i^2\Psi_T^2)/(\Psi_T^2)$; (ii) nonphysical negative density values appear in the long-range region.

Regarding the point (i), the reason for this unbounded variance can be understood if we look at the behavior of the wave function as an electron $\mathbf{r}_i$ approaches the nucleus A with total charge Z_A. The exact wave function in this limit should satisfy the electron−nucleus cusp condition so that

$$\Psi_T^2 \sim_{\mathbf{r}_i \to \mathbf{R}_A} (1 - Z_A|\mathbf{r}_i - \mathbf{R}_A|)^2 \tag{23}$$

This condition is satisfied by the JAGP through the Jastrow one-body factor and leads to the condition that as $\mathbf{r}_i \to \mathbf{R}_A$, the ratio $(\nabla_i^2\Psi_T^2)/(\Psi_T^2)$ becoming proportional to $-(4Z_A)/(|\mathbf{r}_i - \mathbf{R}_A|)$. When calculating the density on a grid point $\mathbf{r}$ near the nucleus $\mathbf{r} \sim \mathbf{R}_A$ the expression (eq 22) will grow as $1/(|\mathbf{r}_i - \mathbf{R}_A|^2)$, thus leading to an unbounded variance.

Both the unbounded variance in the short-range and the appearance of the negative values in the long-range regions can be cured, introducing in eq 22 two additional functions $f(\mathbf{r}_i,\mathbf{r})$ and $g(\mathbf{r})$:[48]

$$\hat{\rho}(\mathbf{r}_i, \mathbf{r}) = -\frac{1}{4\pi} \sum_i^N \left[\frac{1}{|\mathbf{r}_i - \mathbf{r}|} - g(\mathbf{r}) \right] \times \frac{\nabla_i^2 [f(\mathbf{r}_i, \mathbf{r})\Psi_T^2(\mathbf{r}_1, ..., \mathbf{r}_N)]}{\Psi_T^2(\mathbf{r}_1, ..., \mathbf{r}_N)} \tag{24}$$

The function $f(\mathbf{r}_i,\mathbf{r})$ leads to a large reduction of the variance, regularizing the Dirac delta function with no modification of the average value, being a smooth function of $\mathbf{r}_i$ satisfying $f(\mathbf{r}_i = \mathbf{r}; \mathbf{r}) = 1$. The aim of the introduction of the $g(\mathbf{r})$ function is to reduce density fluctuations in the $|\mathbf{r}| \to +\infty$ regime and to avoid negative density values. The VMC average of the improved density estimator therefore becomes

$$\rho(\mathbf{r}) = \left\langle -\frac{1}{4\pi} \sum_i^N \left[\frac{1}{|\mathbf{r}_i - \mathbf{r}|} - g(\mathbf{r}) \right] \frac{\nabla_i^2 [f(\mathbf{r}_i; \mathbf{r})\Psi_T^2(\mathbf{r}_1, ..., \mathbf{r}_N)]}{\Psi_T^2(\mathbf{r}_1, ..., \mathbf{r}_N)} \right\rangle_{\Psi_T^2} \tag{25}$$

with $f(\mathbf{r}_i;\mathbf{r})$ and $g(\mathbf{r})$ defined in ref 48.

We describe briefly below an explicit generalization of such an approach to a molecular system containing M nuclei.

Following the work of Assaraf et al.,[48] we define short- and long-terms for the one-nucleus $f(\mathbf{r})$:

$$f_{SR} = 2Z_A(|\mathbf{r}_i - \mathbf{R}_A| - |\mathbf{r} - \mathbf{R}_A|)$$
$$f_{LR} = (1 + \lambda|\mathbf{r}_i - \mathbf{r}|)e^{-\lambda|\mathbf{r}_i - \mathbf{r}|} \tag{26}$$

and we introduce two one-center weighting coefficients K_S^A and K_L^A for short- and long-range terms, respectively. The one-nucleus function $f(\mathbf{r}_i,\mathbf{r})$ takes in our case the following form

$$f(\mathbf{r}_i, \mathbf{r}) = 1 - K_L^A + K_S^A f_{SR} + K_L^A f_{LR} \tag{27}$$

where the coefficients K_S^A and K_L^A correspond, respectively, to a descending and an ascending Hill function of the distance $|\mathbf{r} - \mathbf{R}_A|$

$$K_S^A = \frac{K^n}{K^n + |\mathbf{r} - \mathbf{R}_A|^n} \tag{28}$$

$$K_L^A = \frac{|\mathbf{r} - \mathbf{R}_A|^n}{K^n + |\mathbf{r} - \mathbf{R}_A|^n} \tag{29}$$

K is the switching point, and n is related to the steepness of the Hill functions, i.e., the higher n the steeper the function. In the neighborhood of nucleus A, i.e., $\mathbf{r} \sim \mathbf{R}_A$, the coefficient K_S is approximated by 1 and K_L by 0; the opposite is verified when the distance $|\mathbf{r} - \mathbf{R}_A|$ is greater than the threshold value K.

In a many-nuclei case, $f(\mathbf{r}_i,\mathbf{r})$ is generalized by adding short-range terms for each nucleus with corresponding weighting coefficients K_S^A, while K_L is defined by the product of the K_L^A functions defined for each nucleus:

$$K_L = \prod_A^M K_L^A = \prod_A^M \frac{|\mathbf{r} - \mathbf{R}_A|^n}{K^n + |\mathbf{r} - \mathbf{R}_A|^n} \tag{30}$$

Finally, the M-nuclei formula for $f(\mathbf{r}_i,\mathbf{r})$ is written as follows:

$$f(\mathbf{r}_i, \mathbf{r}) = 1 - K_L + \sum_A^M K_S^A f_{SR}^A + K_L f_{LR} \tag{31}$$

The general definition has the property of satisfying the electron−nuclear cusp condition at each nucleus, continuing to ensure the condition $f(\mathbf{r}_i = \mathbf{r},\mathbf{r}) = 1$.

The $g(\mathbf{r})$ is defined as a piecewise function:

$$g(\mathbf{r}) = \begin{cases} 0 & \text{for} \quad |\mathbf{r} - \mathbf{R}_A| \le K \\ \dfrac{1}{M} \displaystyle\sum_A^M \frac{1}{|\mathbf{r} - \mathbf{R}_A|} & \text{for} \quad |\mathbf{r} - \mathbf{R}_A| > K \end{cases} \tag{32}$$

To test its reliability, we have calculated the density of the ethyne molecule by using both the standard estimator of eq 19 and our extension of the improved estimator;[48] in section 4 we shall show the differences between the two methods in the density profile along the molecular axis.

3. COMPUTATIONAL DETAILS

The electrical and electronic properties of ethyne have been calculated at the fixed experimental equilibrium geometry,[47] corresponding to R_{CC} = 1.203 Å and R_{CH} = 1.062 Å. The core electrons of the two carbon atoms have been described through the scalar-relativistic energy-conserving pseudopotentials (SR-ECP) defined in refs 60 and 61.

Basis Sets. It is well-known that the convergence of the basis set size is crucial for the proper calculation of multipole moments, polarizability, and the charge density of molecules.[2,34] In particular, the inclusion of a large amount of polarization and diffuse atomic basis functions is required to achieve convergence on ethyne quadrupole moment at the CCSD(T) level, employing up to aug-cc-pV6Z and daug-cc-pVQZ Gaussian basis sets.[44] In QMC, the electronic density, and therefore electrical properties, are not only modulated by the atomic basis set of the determinant expansion but also by the Jastrow factor in a complicated way. This issue leads in general to a faster convergence of the electronic properties with respect to the size of the basis sets, when evaluated with QMC wave functions. Basis set convergence will be therefore investigated in the present work for both the determinantal and the Jastrow parts of JAGP. Table 1 collects the AGP basis sets employed for the present work.

Table 1. AGP Basis Sets Used in This Work[a]

AGP	carbon	hydrogen
G1	(5s4p2d)/[3s3p2d]	(4s2p)/[3s2p]
G2	(5s4p2d)/[4s3p2d]	(4s2p)/[3s2p]
G3	(6s5p2d)/[3s3p2d]	(5s3p2d)/[3s2p2d]
G4	(6s5p2d)/[4s3p2d]	(5s3p2d)/[3s2p2d]
S1	(3s2s*2p2p*2d*)/[3s3p2d]	(2s2s*2p*)/[3s2p]
S2	(3s2s*2p2p*2d*)/[4s3p2d]	(2s2s*2p*)/[3s2p]

[a]The * corresponds to a STO (see text for details).

All the variational parameters of the determinantal and Jastrow basis sets are optimized during our computational procedure as described in the next paragraph. Anyway, a reasonable starting point is essential to improve convergence and guarantee consistency. Starting points for Gaussian primitives are taken as described in the following.

G1 and G2 are the Gaussian basis taken from the aug-cc-pVDZ contraction;[62] G1 is a simplified version since the inner s orbital of the C atom is removed. In both cases, second valence, polarization, and diffuse GTOs are uncontracted orbitals. G3 and G4 have a double-ζ contraction with aug-cc-pVTZ primitives; they have the same contraction of G1 and G2, respectively (G3 misses the inner s orbital like G1), but the second valence orbital for carbon is now a contraction of two primitives, while the diffuse term remains uncontracted. D functions are added to hydrogen according to the triple-ζ scheme.

S1 and S2 are the hybrid GTO/STO basis analogous to G1 and G2; in this case, STOs are used exclusively for uncontracted second valence, polarization, and diffuse terms while the same Gaussian contraction as before describes the valence region. The initial guess for the Slater exponents is given by the corresponding Gaussian through the relation $\zeta_S = (2\zeta_G)^{1/2}$, with ζ_S and ζ_G being the exponents of the STO and of the GTO, respectively; all primitives with $\zeta_G > 10$ are neglected because of the use of a pseudopotential, which also helps for a more stable and efficient optimization procedure. The use of such a hybrid approach improves the long-range description of the wave function and it has been already successfully used for calculating energies of small diatomic molecules.[63,64]

The atomic basis for J_3 (eq 11) has been chosen to be 1s1p for the hydrogen. Three different J_3 basis sets have been chosen for carbon: 1s1p, 2s1p, and 3s2p1d. Uncontracted GTOs are used for each J_3 basis sets. The convergence properties of several quantities, such as the energy, the mean polarizability $\bar{\alpha}$ and its anisotropy $\Delta\alpha$ (eqs 14 and 15), and the mean quadrupole Θ_{eff} (eq 18), will be investigated as a function of the various Jastrow J_3 and AGP basis sets. In particular, the expansion of the AGP basis set has the double effect to improve the atomic basis and to increase the multideterminantal nature of the wave function. In the case of ethyne, where a single-determinant should be able to correctly describe the polarizability,[2,31,34] the effect of the increasing of the basis set would be essentially related to the improvement of the atomic basis due to the introduction of additional polarization and diffuse terms.

Optimization Procedure. The optimization of the wave function parameters has been performed by applying the linear optimization method introduced in refs 14 and 22. The optimization procedure involves a large number (thousands) of variational parameters involving both the determinant of geminal functions (AGP) and Jastrow terms. To improve convergence and to enforce consistency in the optimization procedure, we used a defined protocol that includes several partial steps before fully relaxing all parameters together. In the following seven steps, starting from the initial conditions described in the previous paragraph and from a diagonal $\lambda_{\mu_A\nu_B}$ matrix (eq 7), we allow the optimization algorithm to change the two-body Jastrow term J_2 (eq 9) together with (1) the $\lambda_{\mu_A\nu_B}$ matrix of the AGP (eq 7); (2) the $\lambda_{\mu_A\nu_B}$ matrix and linear coefficients of the atomic orbitals in the AGP; (3) the $\lambda_{\mu_A\nu_B}$ matrix and linear coefficients + exponents of atomic orbitals in the AGP; (4) the $g_{\mu_A\nu_B}$ matrix of J_3, defined in eqs 10 and 11; (5) the $g_{\mu_A\nu_B}$ matrix and linear coefficients + exponents of atomic orbitals in the J_3; (6) all linear parameters (AGP + J); (7) all (linear + exponents) parameters (AGP + J).

The choice of a diagonal $\lambda_{\mu_A\nu_B}$ matrix (e.g., the atomic limit) as a starting point represents a reasonable and unbiased choice as the optimizer is able to rapidly find the correct off-diagonal elements; moreover, the choice of a specific initial guess for J_3 does not significantly affect the minimization pathway. In general, our optimization scheme has been seen to be robust with respect to the starting values of the parameters.

Steps 1−3 first involve the optimization of the coupling matrix of the AGP[20] and then the atomic basis is modified, with a fixed J_3; on the contrary, steps 4 and 5 are characterized by the optimization of the J_3 parameters, in the presence of the new AGP. Finally, with steps 6 and 7, we release all the parameters by performing a full wave function optimization. The role of these steps on the convergence of the electrical properties of ethyne will be also addressed in the next section.

Electronic Density. For the improved estimator we have chosen $\lambda = 1.9$, the average between the values for H and C ($\lambda_H = 2.0$ and $\lambda_C = 1.8$), in order to take into account the long-range behavior of both atoms; the switching point in the Hill functions (eqs 28 and 29) is equal to 0.017 bohr in order to guarantee a finite variance on the nuclei and a reduced variance in the other regions and a steepness given by a $n = 4$ power.

4. RESULTS AND DISCUSSION

We have studied the convergence of isotropic polarizability $\bar{\alpha}$ and of its anisotropy $\Delta\alpha$ as a function of the AGP basis sets described in Table 1 in combination with three different three-body Jastrow factors J_3 of increasing size. As described in the previous section, we have used GTO-based basis sets (G1-G4) and mixed GTO/STO basis sets (S1 and S2) with different contraction schemes. The difference between G1-G2 and G3-G4 results in the number of primitives and in the presence of d functions on H atoms. G2 and G4 have a larger number of primitives with respect to G1 and G3, respectively. S1 and S2 are taken from G1 and G2, substituting the uncontracted orbitals of polarization and diffuse character with Slater functions.

All results are reported in Table 2 together with the total number of variational parameters N_P of the wave function.

Table 2. AGP Convergence of $\bar{\alpha}$, $\Delta\alpha$, and the Variational Energy E_{VMC}[a]

AGP/J_3 = 1s1p	N_P	$\bar{\alpha}$ [au]	$\Delta\alpha$ [au]	E_{VMC} [Hartree]
G1	2183	20.34(1)	16.91(4)	−12.4692(1)
G2	2322	20.98(1)	13.85(4)	−12.4750(1)
G3	3661	22.33(1)	11.68(4)	−12.4691(1)
G4	3840	22.55(1)	12.23(4)	−12.4751(1)
S1	2183	21.00(1)	11.93(4)	−12.4708(1)
S2	2322	22.82(1)	13.51(4)	−12.4725(1)
AGP/J_3 = 2s1p	N_P	$\bar{\alpha}$	$\Delta\alpha$	E_{VMC}
G1	2222	22.24(1)	14.77(4)	−12.4671(1)
G2	2361	22.22(1)	12.78(4)	−12.4756(1)
G3	3700	22.85(1)	13.24(4)	−12.4670(1)
G4	3879	22.87(1)	11.36(4)	−12.4755(1)
S1	2222	22.75(1)	14.18(4)	−12.4742(1)
S2	2361	22.62(1)	13.12(4)	−12.4747(1)
AGP/J_3 = 3s2p1d	N_P	$\bar{\alpha}$	$\Delta\alpha$	E_{VMC}
G1	2741	22.15(1)	12.45(4)	−12.4796(1)
G2	2880	22.16(1)	11.83(4)	−12.4830(1)
G3	4219	22.65(1)	11.20(4)	−12.4789(1)
G4	4398	22.59(1)	12.90(4)	−12.4843(1)
S1	2741	22.41(1)	13.19(4)	−12.4828(1)
S2	2880	22.57(1)	12.47(4)	−12.4816(1)

[a]AGP convergence of $\bar{\alpha}$, $\Delta\alpha$, and the variational energy E_{VMC} at zero field, using different basis sets for the AGP and for the carbon J_3 Jastrow term. All the quantities are in au. N_P is the total number of parameters of Ψ_T.

They include the two-body Jastrow (only one parameter), all atomic parameters (linear coefficients and exponents) of the AGP and J_3 basis sets, and the coupling matrices of AGP and J_3 (eqs 7 and 11).

The upper part of Table 2 collects the AGP convergence for the smallest Jastrow basis J_3 = 1s1p. The right column of Table 2 shows the variational VMC energy of the molecule at zero external field. The number of AGP contractions in the carbon atom description plays an important role in the absolute variational energy: G2-G4 energies are indeed lower than G1-G3. On the other hand, no significant differences are reported if GTO primitives are added, from G1 to G3 and from G2 to G4, within the same contraction. A similar behavior is also found for the S series. As expected, the calculation of the polarizability turns out to be more sensitive to the basis set. $\bar{\alpha}$ is clearly underestimated in G1-G2, and $\Delta\alpha$ undergoes large fluctuations passing from one basis set to another.

Interestingly, the use of a larger Jastrow factor, J_3 = 2s1p, as shown in the middle part of Table 2, significantly reduces the dependence of the polarizability from the AGP basis set. All calculated values are within 0.6 au, regardless if GTO or mixed GTO/STO basis sets are considered. $\Delta\alpha$ values are still less stable over the data set. A difference with respect to the previous case is found for the mixed GTO/STO basis sets since they converge independently of the number of primitives on the carbon atoms and polarization functions on the hydrogen atoms. The largest double-ζ Jastrow factor J_3 = 3s2p1d for the carbon atom further improves the quality of the variational convergence of E_{VMC}, as evident in the lower part of Table 2.

The high accuracy of the JAGP wave function has been validated comparing the VMC energies for the two largest basis sets with LRDMC energies. The calculated LRDMC ground state energies are −12.4927(2) and −12.4931(2) Hartree for G4(3s2p1d) and S2(3s2p1d) basis sets, respectively. The variational ansatzs are only about 10 mH higher in energy (see Table 2), confirming the good quality of the optimized trial wave functions, as already reported by ref 8. LRDMC calculations have been carried out with $a = 0.1$ bohr.

The differences in the polarizabilities is further reduced along the AGP basis set series, leading to the value of 22.59 au for the larger G4 basis set. Also the estimate of $\Delta\alpha$ is more rapidly converging toward the G4 and S2 values, namely, 12.90(4) au and 12.47(4) au, respectively. The effect of the application of more complex Jastrow factors is summarized in the graph of Figure 1. The G1, G2, and S1 basis sets are quite sensitive to

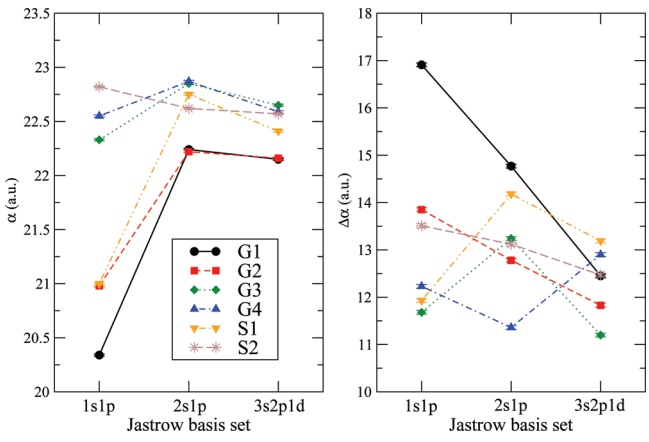

Figure 1. $\bar{\alpha}$ and $\Delta\alpha$ as a function of the size of the J_3 Jastrow basis set (for the carbon atom) for the AGP basis sets used in the present work.

the applied J_3, showing a clear convergence in $\bar{\alpha}$ and in $\Delta\alpha$ when moving from the smaller 1s1p to the larger 3s2p1d J_3; the more accurate AGP functions G3, G4, and S2 are instead characterized by a smaller dependence, even though the evolution of $\Delta\alpha$ for G3 is similar to the S1 one.

To understand the role of some specific parameters of the trial wave function Ψ_T in the determination of the polarizability, we may follow the evolution of $\bar{\alpha}$ and $\Delta\alpha$ along the

dx.doi.org/10.1021/ct300171q | J. Chem. Theory Comput. 2012, 8, 1952−1962

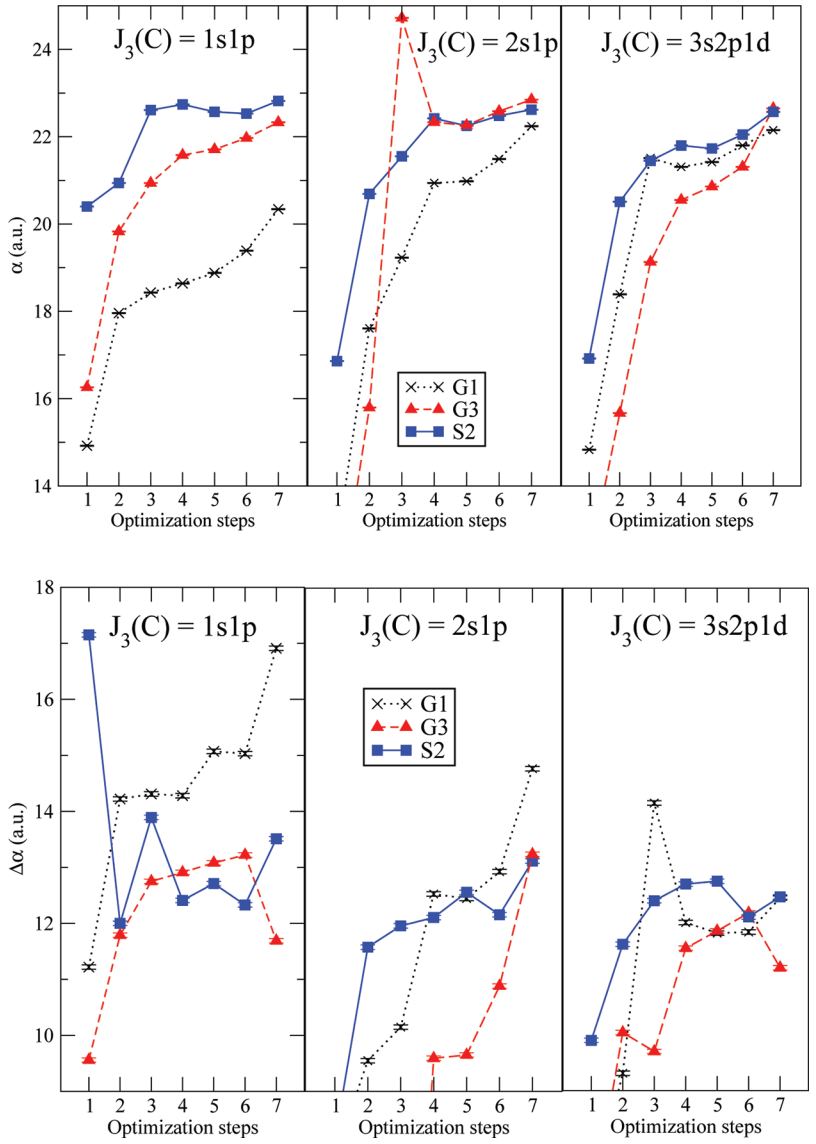

Figure 2. Evolution of $\bar{\alpha}$ (upper panel A) and $\Delta\alpha$ (lower panel B) during the Ψ_T optimization steps (see section 3). G1, G3, and S2 basis sets, coupled with three-body Jastrow 1s1p, 2s1p, and 3s2p1d for carbon, are shown.

optimization procedure by calculating such quantities at intermediate steps of our optimization scheme. At every optimization step only a given subset of parameters has been optimized, as described in the previous section. Three different AGP basis sets (G1, G3 and S2) are reported in Figure 2 in combination with all three J_3.

The convergence of $\bar{\alpha}$ (panel A) underlines how steps 2, 3, and 4, which are the optimization of the exponents of the AGP atomic basis set, of the full AGP determinant, and of the J_3 coupling matrix, are relevant to achieve a robustness of the value with respect to the AGP basis set. In panel B, the behavior of $\Delta\alpha$ with different Jastrow factors clearly shows that step number 7 (all the parameters optimized at once) is an important task to have a more consistent value along the different AGP basis sets. In summary, we observe that the application of a large Jastrow term reduces the differences coming from the AGP basis, leading to a more compact, almost AGP-independent convergence for the polarizability values. The analysis of the convergence along the optimization steps revealed that the full relaxation of all wave function parameters, including linear and nonlinear coefficients of Jastrow and AGP basis sets, is crucial for the achievement of convergence using such compact functional form.

At variance with what we have found for $\bar{\alpha}$ and $\Delta\alpha$, the VMC estimate of Θ_{eff} is not dramatically affected by the choice of the atomic orbital type. As one can see, for instance, in the left column of Table 3, where we show the results for the different AGP basis coupled with the smallest J_3 basis 1s1p for the

Table 3. Effective Traceless Quadrupole Θ_{eff} in VMC

AGP/J_3 = 1s1p	Θ_{eff} [au]	AGP/J_3 = 2s1p	Θ_{eff} [au]	AGP/J_3 = 3s2p1d	Θ_{eff} [au]
G1	4.964(1)	G1	4.888(1)	G1	4.847(1)
G2	5.172(1)	G2	5.052(1)	G2	5.095(1)
G3	5.094(1)	G3	4.999(1)	G3	4.843(1)
G4	5.049(1)	G4	5.076(1)	G4	5.080(1)
S1	5.108(1)	S1	5.032(1)	S1	5.104(1)
S2	5.061(1)	S2	5.068(1)	S2	5.009(1)

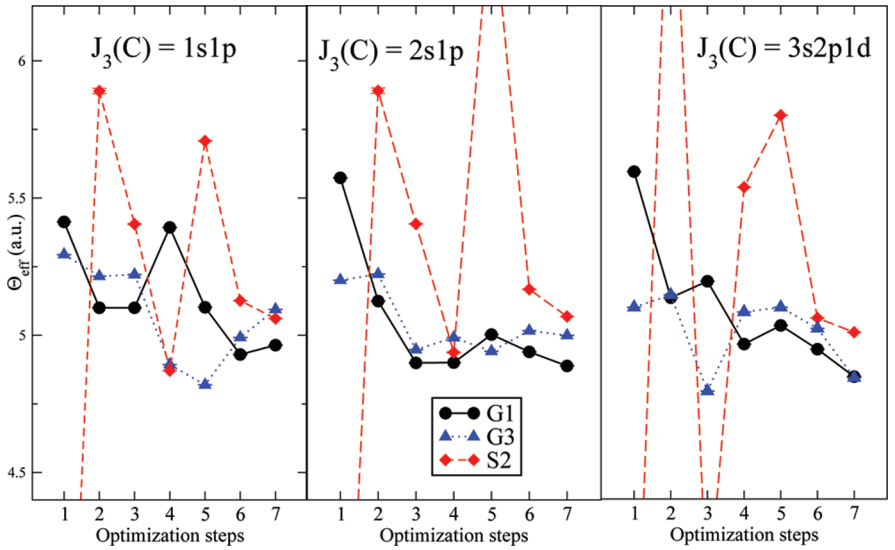

Figure 3. Evolution of Θ_{eff} during the Ψ_T optimization (see section 3). G1, G3, and S2 basis sets, coupled with three-body Jastrow 1s1p, 2s1p, and 3s2p1d for carbon, are shown.

carbon, the converged value seems to be quite insensitive to the use of GTOs or STOs.

The above finding is confirmed looking at the central column of Table 3 where Θ_{eff} moves from 4.888(1) [G1(2s1p)] to 5.076(1) [G4(2s1p)] au; moreover, passing from 1s1p to 2s1p J_3 indicates that the use of a more complex Jastrow factor does not produce evident modifications in the Θ_{eff} values, even if smaller differences among the basis sets are found. The use of a double-ζ 3s2p1d J_3 does not change the previous findings; the right column of Table 3 confirms the fact that the evaluation of the quadrupole moment does not strictly depend on the particular combination of AGP and J_3 factors. Θ_{eff} turned out to be rather sensitive to the partial optimization steps as shown in Figure 3, in particular to the optimization of the Jastrow factor parameters, which are fine modulating the electron density.

The accuracy of the present QMC values depends on the quality of the trial wave function Ψ_T and on how large the variational parameters space is; N_P doubles moving from the smallest G1(1s1p) to the biggest G4(3s2p1d) wave function (see Table 2). Especially in the case of the polarizability, our study points out the fact that accurate values can be reached by using mixed GTO/STO AGP basis sets (S1 and S2, with a variational space less than 3000 parameters), comparable with those obtained along the G series but with a consistently reduced computational effort.

Electrical properties like the polarizability and quadrupole moment require large basis sets with spdf character in CC and DFT calculations;[2,34,44] Table 4 shows that convergence in polarizability for DFT/B3LYP (which is known to overestimate $\bar{\alpha}$) needs larger basis sets than those used in the present work.

Table 5 reports several data from literature for $\bar{\alpha}$ and $\Delta\alpha$; HF (23.219, 12.026 au) and MP2 (23.162, 12.197 au), (23.033, 12.112 au) values[2] have been corrected by the contribution of the fundamental vibrational state. $\Delta\alpha$ is estimated, from both experimental and theoretical standpoints, between 11.5(6)[2] and 13(1) au.[34] We also corrected our results by applying the MP2 zero-point-energy corrections reported by ref 2 to G4(3s2p1d) and S2(3s2p1d), corresponding to 0.451 au for $\bar{\alpha}$ and 0.543 au for $\Delta\alpha$, respectively.

In Table 6, a collection of the state-of-art for the HCCH quadrupole is shown, and some of the calculated estimates have

Table 4. $\bar{\alpha}$ and $\Delta\alpha$ Convergence for B3LYP Calculations

B3LYP	$\bar{\alpha}$ [au]	$\Delta\alpha$ [au]
cc-pVDZ	16.16	19.19
cc-pVTZ	19.72	16.19
cc-pVQZ	21.70	14.33
cc-pv5Z	22.55	13.71
aug-cc-pVDZ	23.26	13.14
aug-cc-pVTZ	23.81	12.31
aug-cc-pVQZ	23.93	12.05
aug-cc-pv5Z	23.95	11.99

been averaged on the vibrational ground-state; in both cases a direct comparison with our converged VMC estimates is proposed, corresponding to the G4(3s2p1d) and S2(3s2p1d) wave functions, corrected by the vibrational ground-state contribution, −0.0812 au with MP2/TZP2(f).[2]

The VMC α results lie in the experimental range and well agree with the other correlated methods. VMC $\Delta\alpha$ is slightly overestimated and we are not able to identify a full and clear convergence as a function of AGP and J_3 basis sets, as shown in the lower panel of Figure 2. Additionally, LRDMC mixed estimates for G4(3s2p1d) and S2(3s2p1d) wave functions are reported for the polarizability and the quadrupole moment (Tables 5 and 6), confirming the reliability of VMC calculations; LRDMC results for $\Delta\alpha$ give a smaller value than the VMC ones, in better agreement with the other methods and in the middle of the scattering of the experimental data (Table 5).

The last ethyne property studied in this work is the charge density distribution along the molecular axis. The unidimensional VMC density profile is reported in Figure 4, where a comparison between the standard (eq 19) and our improved estimator, defined in section 2.4, is shown. We used an all-electron calculation with the G2(2s1p) wave function (no cutoff for ζ_G values is applied) has been performed.

The graph shows how the new estimator dramatically improves the quality of the density profile either along the CC and CH bonds; starting by the same sampled points and using the same spatial grid, noise and error bars are considerably reduced.

Table 5. Ethyne $\bar{\alpha}$ and $\Delta\alpha$

$\bar{\alpha}$ [au]	$\Delta\alpha$ [au]	method	$\bar{\alpha}$ [au]	$\Delta\alpha$ [au]	method
23.11	12.34	HF[31]		13(1)	Exp.[34]
22.716	11.474	HF[2]	22.67(23)	11.81(35)	Exp.[28]
23.219	12.026	HF[a2]		11.95(36)	Exp.[29]
21.51	13.83	MP2[33]		11.5(6)	Exp.[2]
22.711	11.654	MP2[2]		12.09	Exp.[38]
23.162	12.197	MP2[a2]	23.53(25)		Exp.[42]
23.033	12.112	MP2[a2]	22.9		Exp.[25]
22.52	11.58	CCSD[34]	22.5		Exp.[26]
22.3		Exp.[26]	22.7		Exp.[28]
22.95		Exp.[36]	26.5		Exp.[27]
23.04(1)	13.44(4)	VMC[b]	23.02(1)	13.01(4)	VMC[c]
23.29(4)	12.25(7)	LRDMC[b]	23.25(4)	11.79(7)	LRDMC[c]

[a]Corrected by the vibrational ground state contribution. [b]G4(3s2p1d). [c]S2(3s2p1d) corrected by MP2/TZP2(f) vibrational estimate.[2]

Table 6. Ethyne Quadrupole Moments

Θ [au]	method	Θ [au]	method
5.2476	HF[2]	4.795	QCISD(T)[2]
5.2090	HF[a2]	4.714[a]	QCISD(T)[2]
5.444	HF[44]	4.717	MRCI[39]
5.05, 5.24	HF[41]	4.88	MP4[35]
5.460	HF[34]	4.9381	CCSD[43]
4.8530	MP2[2]	4.910	CCSD[46]
4.7718	MP2[a2]	4.8715	CCSD(T)[43]
4.8602	MP2[43]	4.71	Exp.[2]
4.787	MP4[2]	4.48	Exp.[37]
4.706	MP4[a2]	5.57	Exp.[30]
4.907	DFT (B3LYP)[46]	4.03	Exp.[32]
4.890	DFT (B3LYP)[44]	4.65(18)	Exp.[43]
4.999(1)	VMC[b]	4.928(1)	VMC[c]
5.022(2)	LRDMC[b]	4.921(2)	LRDMC[c]

[a]Corrected by the vibrational ground state contribution. [b]G4(3s2p1d). [c]S2(3s2p1d) corrected by MP2/TZP2(f) vibrational estimate.[2]

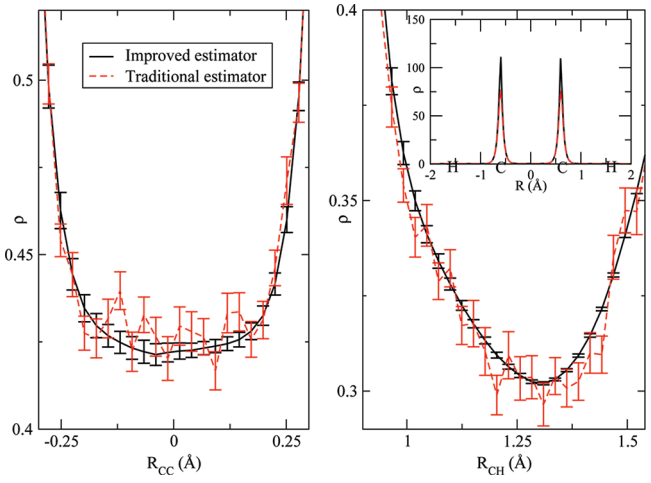

Figure 4. Comparison between the traditional density estimator (eq 19) (red, dashed line) and the improved one defined in section 2.4 (black, continuous line), for the CC and CH bonds; the full all-electron radial density is shown in the inset. Calculations from an all-electron optimization of the G2(2s1p) wave function.

5. CONCLUSIONS

The polarizability, the quadrupole moment and the charge density of ethyne have been calculated at VMC and LRDMC level on a experimentally determined geometry, by means of the JAGP trial wave function, composed by a AGP determinantal part and a Jastrow factor. Detailed investigation on the basis sets has resulted in the study of the convergence of such properties increasing the complexity of the AGP and of J_3 parts of the wave function. Results for $\bar{\alpha}$ and Θ_{eff} well match with the data available in literature, from both experimental measurements and *ab initio* calculations, and are demonstrated to be well converged when looking at the comparison between VMC and LRDMC values. VMC calculations seem instead to slightly overestimate the polarizability anisotropy $\Delta\alpha$ with respect to the LRDMC results.

The use of an extended Jastrow factor is important to achieve convergences already with relatively small basis sets for the AGP. Our analysis indicates that the full optimization of the atomic orbitals, exponents included, is a key ingredient for obtaining converged results and that a compromise between the variational space size and the accuracy of results must be found in order to make the quality of Ψ_T and the computational effort reasonable. The number of variational parameters can be reduced if a mixed GTO/STO wave function is used, as already shown in refs 63 and 64 for the energetics of atoms and small diatomic molecules; the application of STO functions is here extended to the study of the polarizability, the quadrupole moment, and the charge density of the ethyne. Second valence, polarization, and diffuse terms of the AGP basis are described by STO functions and a faster convergence is achieved for the smallest wave functions employed here with respect to the related Gaussian ones, on the other hand a full convergence in the AGP and Jastrow space is found for the Gaussian series. A clear improvement in the description of the density is shown when the new estimator is used, in contrast with the noisy profile obtained with the traditional density estimator, thus leading to a very smooth density profile even in poorly sampled regions.

In this work we have shown that a simple correlated variational ansatz is able to provide state-of-the-art polarization properties of ethyne, with relatively small basis sets and, by consequence, a limited computational effort. LRDMC calculations show that the VMC results presented here are already accurate enough, within the present experimental uncertainty. In view of the application of this approach to much larger

systems, VMC seems to be a good compromise between accuracy and efficiency, since it is characterized by a better scaling with respect to the number of electrons, if compared to LRDMC.

In conclusion, our results demonstrate that Variational Monte Carlo methods are able to obtain precise molecular polarizabilities and multipole moments using a rather compact wave function, therefore opening the way to the accurate study of electrical properties of larger systems.

AUTHOR INFORMATION

Corresponding Author

*E-mail: leonardo.guidoni@univaq.it.

Present Address

[‖]Center for Integrative Bioinformatics Vienna (CIBIV), Max F. Perutz Laboratories (MFPL), Dr. Bohr Gasse 9 A-1030, Wien, Austria.

Notes

The authors declare no competing financial interest.

ACKNOWLEDGMENTS

We acknowledge CASPUR and CINECA supercomputing centers and the PRACE Project No. PRA053 for computational resources. We thank Donato Pera and Piergiacomo De Ascaniis of the Department of Pure and Applied Mathematics of the University of L'Aquila for the technical support. L.G., E.C., and M.B. acknowledge funding provided by the European Research Council Project No. 240624 within the VII Framework Program of the European Union.

REFERENCES

(1) Maitland, G. C.; Rigby, M.; Smith, E. B.; Wakeham, W. A. *Intermolecular Forces*; Oxford University Press: Oxford, U.K., 1981.
(2) Russell, A. J.; Spackman, M. A. *Mol. Phys.* **1996**, *88*, 1109.
(3) Hammond, B. L.; Lester, W. A., Jr.; Reynolds, P. J. *Monte Carlo Methods in Ab-Initio Quantum Chemistry*; World Scientific: River Edge, NJ, 1994.
(4) Foulkes, W. M. C.; Mitas, L.; Needs, R. J.; Rajagopal, G. *Rev. Mod. Phys.* **2001**, *73*, 33.
(5) Ceperley, D. M. *Rev. Mod. Phys.* **1995**, *67*, 279.
(6) Baroni, S.; Moroni, S. *Phys. Rev. Lett.* **1999**, *82*, 4745.
(7) Towler, D. M. In *Computational Methods for Large Systems*; Wiley: Hoboken, NJ, 2011; p 119.
(8) Barborini, M.; Sorella, S.; Guidoni, L. *J. Chem. Theory Comput.* **2012**, *8*, 1260−1269.
(9) Reynolds, P. J.; Ceperley, D. M.; Alder, B. J.; Lester, W. A., Jr. *J. Chem. Phys.* **1982**, *77*, 5593.
(10) Kolorenc, J.; Mitas, L. *Rep. Prog. Phys.* **2001**, *74*, 026502.
(11) Spanu, L.; Sorella, S.; Galli, G. *Phys. Rev. Lett.* **2009**, *103*, 196401.
(12) Maezono, R.; Drummond, N. D.; Ma, A.; Needs, R. J. *Phys. Rev. B* **2010**, *82*, 184108.
(13) Sterpone, F.; Spanu, L.; Ferraro, L.; Sorella, S.; Guidoni, L *J. Chem. Theor. Comput.* **2008**, *4*, 1428.
(14) Sorella, S.; Casula, M.; Rocca, D. *J. Chem. Phys.* **2007**, *127*, 14105.
(15) Schautz, F.; Filippi, C. *J. Chem. Phys.* **2004**, *120*, 10931.
(16) Zimmermann, P. M.; Toulouse, J.; Zhang, Z.; Musgrave, C. B.; Umrigar, C. J. *J. Chem. Phys.* **2009**, *131*, 124103.
(17) Filippi, C.; Buda, F.; Guidoni, L.; Sinicropi, A. *J. Chem. Theor. Comput.* **2012**, *8*, 112.
(18) Sorella, S. TurboRVB Quantum Monte Carlo package. http://people.sissa.it/~sorella/web/index.html, accessed April 1, 2012.
(19) Casula, M.; Sorella, S. *J. Chem. Phys.* **2003**, *119*, 6500.
(20) Casula, M.; Attaccalite, C.; Sorella, S. *J. Chem. Phys.* **2004**, *121*, 7110.
(21) Sorella, S. *Phys. Rev. B* **2005**, *71*, 241103(R).
(22) Toulouse, J.; Umrigar, C. J. *J. Chem. Phys.* **2007**, *126*, 084102.
(23) Petruzielo, F. R.; Toulouse, J.; Umrigar, C. J. *J. Chem. Phys.* **2011**, *134*, 064104.
(24) Li, Y.; Vrbik, J.; Rothstein, S. M. *Chem. Phys. Lett.* **2007**, *445*, 345.
(25) Waatson, H. E.; Ramaswarmy, K. L. *Proc. R. Soc. London* **1936**, *A 156*, 130.
(26) Stuart, H. A. *Atom und Molekularphysik*; Springer: Berlin, Germany, 1951.
(27) Maryott, A. A.; Buckley, F. U.S. National Bureau of Standards Circular No. 537; U.S. Government Printing Office: Washington, DC, 1953.
(28) Alms, G. R.; Burnham, A. K.; Flygare, W. H. *J. Chem. Phys.* **1975**, *63*, 3321.
(29) Bogaard, M. P.; Buckingham, A. D.; Pierens, R. K.; White, A. H. *J. Chem. Soc. Faraday Trans. 1* **1978**, *74*, 3008.
(30) King, H.; Gerschka, H.; Huttner, W. *Chem. Phys. Lett.* **1983**, *96*, 631.
(31) Jamison, C. J.; Fowler, P. W. *J. Chem. Phys.* **1986**, *85*, 3432.
(32) Dagg, I. R.; Anderson, A.; Smith, W.; Missio, M.; Joslin, C. G.; Read, L. A. *Can. J. Phys.* **1988**, *66*, 453.
(33) Spackman, M. A. *J. Phys. Chem.* **1989**, *93*, 7594.
(34) Maroulis, G.; Thakkar, A. J. *J. Chem. Phys.* **1990**, *93*, 652.
(35) Maroulis, G. *Chem. Phys. Lett.* **1991**, *177*, 352.
(36) Kumar, A.; Meath, W. J. *Mol. Phys.* **1992**, *75*, 311.
(37) Coonan, M. H.; Ritchie, L. D. *Chem. Phys. Lett.* **1993**, *202*, 237.
(38) Barnes, J. A.; Gough, T. E.; Stoer, M. *Chem. Phys. Lett.* **1995**, *237*, 437.
(39) Bündgen, P.; Grein, F.; Thakkar, A. J. *J. Mol. Struct.* **1995**, *305*, 7.
(40) Watson, J. N. Ph.D. Thesis, University of New England, Armidale NSW, Australia, 1995.
(41) deLuca, G.; Russo, N.; Sicilia, E.; Toscano, M. *J. Chem. Phys.* **1996**, *105*, 3206.
(42) Olney, T. N.; Cann, N. M.; Cooper, G.; Brion, C. E. *Chem. Phys.* **1997**, *223*, 59.
(43) Halkier, A.; Coriani, S. *Chem. Phys. Lett.* **1999**, *303*, 408.
(44) Gearhart, D. J.; Harrison, J. F.; Hunt, K. L. C. *Int. J. Quantum Chem.* **2003**, *95*, 697.
(45) Neugebauer, A.; Häfelinger, G. *J. Phys. Org. Chem.* **2006**, *19*, 196.
(46) Harrison, J. F. *J. Chem. Phys.* **2010**, *134*, 214103.
(47) Lievin, J.; Demaison, J.; Herman, M.; Fayt, A.; Puzzarini, C. *J. Chem. Phys.* **2011**, *134*, 064119.
(48) Assaraf, R.; Caffarel, M.; Scemama, A. *Phys. Rev. E* **2007**, *75*, 035701.
(49) Casula, M.; Filippi, C.; Sorella, S. *Phys. Rev. Lett.* **2005**, *95*, 100201.
(50) Casula, M.; Moroni, S.; Sorella, S.; Filippi, C. *J. Chem. Phys.* **2010**, *132*, 154113.
(51) Pauling, L. *The Nature of the Chemical Bond*, 3rd ed.; Cornell University Press: Ithaca, NY, 1960.
(52) Pople, J. A. *Proc. R. Soc. London, Ser. A* **1950**, *202*, 323.
(53) Hurley, A. C.; Lennard-Jones, J. E.; Pople, J. A. *Proc. R. Soc. London, Ser. A* **1953**, *220*, 446.
(54) Marchi, M.; Azadi, S.; Sorella, S. *Phys. Rev. Lett.* **2011**, *107*, 086807.
(55) Beaudet, T. D.; Casula, M.; Kim, J.; Sorella, S.; Martin, R. *J. Chem. Phys.* **2008**, *129*, 164711.
(56) Drummond, N. D.; Towler, M. D.; Needs, R. J. *J. Phys. Rev. B* **2004**, *70*, 234119.
(57) Marchi, M.; Azadi, S.; Casula, M.; Sorella, S. *J. Chem. Phys.* **2009**, *131*, 154116.
(58) Kobus, J.; Moncrieff, D.; Wilson, S. *J. Phys. B: At. Mol. Opt. Phys.* **2001**, *34*, 5127.
(59) Buckingam, A. D. *Adv. Chem. Phys.* **1967**, *12*, 107.

(60) Burkatzki, M.; Filippi, C.; Dolg, M. *J. Chem. Phys.* **2007**, *126*, 234105.
(61) Burkatzki, M.; Filippi, C.; Dolg, M. *J. Chem. Phys.* **2008**, *129*, 164115.
(62) Dunning, T. H. *J. Chem. Phys.* **1989**, *90*, 1007.
(63) Filippi, C.; Umrigar, C. J. *J. Chem. Phys.* **1996**, *105*, 213.
(64) Nemec, N.; Towler, M. D.; Needs, R. J. *J. Chem. Phys.* **2010**, *132*, 034111.